

GHZ-TO-THZ BROADBAND COMMUNICATIONS FOR 6G NON-TERRESTRIAL NETWORKS

Akhtar Saeed¹, Hilal Esra Yaldız², Fatih Alagoz³

¹Department of Electrical Engineering, DHA Suffa University, Karachi, Pakistan, ²Electrical and Electronics Engineering Department, Bogazici University, Istanbul, Turkey, ³Department of Computer Engineering, Bogazici University, Istanbul, Turkey

NOTE: Corresponding author: Akhtar Saeed, akhtarsaeed@sabanciuniv.edu

Abstract – Recently, Terahertz (THz) band communications at various atmospheric altitudes have been studied due to larger bandwidth availability and reduced water vapor concentrations at higher atmospheric altitudes as compared to sea level. In this paper, as special cases of 6G aerial communication networks, we consider: (1) Low Altitude Platform-to-High Altitude Platform (LAP-to-HAP), (2) HAP-to-HAP, and (3) HAP-to-Satellite (HAP-to-SAT) GHz-to-THz broadband communications over (1-1000) GHz by analyzing total path loss and total usable bandwidth. For obtaining realistic absorption loss at practical altitudes, we employ the International Telecommunications Union's (ITU) model using the standard weather profile. We consider four practical carrier frequencies offering low absorption loss values i.e., $f_1 = 0.140$ THz (D band: 110–170 GHz), $f_2 = 0.300$ THz (275–325 GHz), $f_3 = 0.750$ THz, and $f_4 = 0.875$ THz for analyzing total path loss. Numerical results show that due to improved atmospheric conditions particularly above 23 km altitudes, increasing the Rx-HAP altitude in HAP-to-HAP communications promises a lower total path loss of up to 7.7 %, even at the cost of an increase in the Tx-Rx-HAP distance from 1 km to 34 km, promising Tbps rates for 6G non-terrestrial communications. Additionally, total usable bandwidth analysis demonstrates that with total antenna gains of 80 dBi, bandwidth in the order of 100s of GHz is usable for the LAP-to-HAP scenario, the entire considered broadband is usable for the HAP-to-HAP scenario between 16 km to 50 km, and the HAP-to-SAT scenario between a HAP at 19 km and SAT at 100 km, truly showcasing the potential of employing GHz-to-THz broadband communications cognitively over (1-1000) GHz for various practical 6G non-terrestrial networks.

Keywords – Absorption loss, broadband, cognitive radios, D Band, high altitude platforms, L band, low altitude platforms, millimeter wave communications, satellite communications, terahertz communications, total path loss, total usable bandwidth

1. INTRODUCTION

Wireless communications have been progressing towards 6G to meet the demand for higher bandwidth and rates as compared to the existing sub-6GHz bands, which are saturated [1]. To meet these demands, higher frequency bands have been considered, such as L Band (1-2) GHz [2], millimeter wave band (28, 60, 73) GHz [3], and terahertz (THz) band (0.1-10 THz) [4]. Among these bands, the THz band is a promising one, offering rates in the order of Tbps, with multiple bandwidths, each several GHz wide, which can be possibly employed for the design and development of 6G and beyond wireless systems [5]. However, THz Electromagnetic (EM) wave is highly affected by absorption loss as it propagates through the atmosphere. This absorption loss is mainly due to water vapor molecules present in the atmosphere [6]. Naturally, the water vapor concentration is maximum at sea level. Therefore, THz communications at sea level are usually limited up to a few meters only [7]. At higher altitudes above the sea level, the water vapor concentration decreases, enabling THz band communications at higher altitudes more feasible [8].

Use cases of employing THz for aerial communications can be multifold. For instance, along with optical and microwave solutions, Inter-Satellite Links (ISLs) over the THz band are presented in [9]. ISL connectivity and in-vivo

nanonetworks are proposed in [10], where THz communications are suggested to allow Vertical Heterogeneous Network (V-HetNet) elements to work in harmony. To savor this harmony, channel models must be accurate. The channel characteristics of the THz band are investigated to map the band's feasibility for aviation [11], where the authors offer a thorough channel model for aerial THz communications that accounts for both the non-flat Earth geometry and the major properties of the frequency-selective THz channel, showing that the capability of the airborne THz link might reach speeds of 50–150 gigabit per second (Gbps). A recent study in [12] has considered THz band (0.1-10) THz wireless communications for new deep space explorations e.g., for Mars-space THz links.

Spectrum management will place an important role in regard to the interference issue in the THz band [13]. A massive THz band can be sufficed for the challenge of spectrum scarcity by allocating sub-bands to individual users, hence, mitigating the interference [14, 15]. A similar approach for drones has been applied in our earlier work [4], where, for instance, a drone base station providing wireless services to other drones can use different sub-bands, each several GHz wide. Subsequently, capacity in the order of several 100s of Gbps is achievable even under beam misalignment fading and multipath fading.

A few recent studies have shown the massive potential of employing the THz band for aerial communications with a substantial performance improvement as compared to the THz communications at sea level. In [13], open research directions for drone networks over the THz band are presented, highlighting issues in channel estimation, physical layer, Ultra-Massive Multiple Input Multiple Output (UM-MIMO), and Mobile Edge Computing (MEC), to name a few. In [4], an extensive analysis of THz band communications of four practical aerial vehicle scenarios is provided for drones, jet planes, high altitude UAVs, and satellites at various practical altitudes, transmission distances, zenith angles, weather profiles, and fading conditions of Multipath (MP) fading and Beam Misalignment (BM) fading. Moreover, common flat bands for frequency-selective path gain and the colored noise spectrums, both of which are heavily impacted by atmospheric circumstances, are calculated using a channel model for aerial communications in the THz band. In [8], total path loss and total usable bandwidth analysis of four identical aerial vehicle scenarios as in [4] are presented over the THz band (0.75-10 THz). The Line-by-Line Radiative Transfer Model (LBLRTM) is employed for obtaining THz absorption loss. In this work, as special instances of [8], the feasibility of GHz-THz broadband communications over (1-1000) GHz for High Altitude Platform (HAP)-to-HAP and HAP-to-Satellite (HAP-to-SAT) is evaluated. Moreover, unlike [8], we consider GHz-THz broadband over (1-1000) GHz to assess total path loss and total usable bandwidth of the aerial communication scenarios by employing the ITU model. Additionally, based on a recent study on net-worked flying platforms studying tethered/non-tethered Low Altitude Platforms (LAPs) [16], we analyze a special case of 6G non-terrestrial networks i.e., LAP-HAP communications. We consider four specific THz center frequencies for analyzing the total path loss at varying altitudes, i.e., $f_1 = 0.140$ THz (D band) and $f_2 = 0.300$ THz as in [17], whereas $f_3 = 0.750$ THz and $f_4 = 0.875$ THz are from [18, 19], all of which are not covered in [8]. Total path loss results over the four considered THz carrier frequencies depict that due to the improved atmospheric conditions particularly above 23 km altitude, HAP-to-HAP communications between 16 km to 17 km ($d = 1$ km) offer lower total path loss values as compared to the HAP-to-HAP communications between 16 km to 50 km ($d = 34$ km), while in all three scenarios, $f_4 = 0.875$ THz offers a lower total path loss as compared to the $f_3 = 0.750$ THz, which is due to the frequency selective of the THz band. Furthermore, total usable bandwidth analysis depicts that with a total antenna gain of 80 dBi, bandwidth in the order of 100s GHz becomes usable for the LAP-to-HAP scenario, whereas the entire considered broadband (1-1000) GHz becomes usable for the HAP-to-HAP scenario between 16 km to 50 km, and the HAP-SAT scenario between a HAP at 19 km and SAT

at 100 km, truly showcasing the potential of employing the GHz-THz broadband communications cognitively over (1-1000) GHz for 6G non-terrestrial networks. The rest of the paper is organized as follows: Section 2 presents the system model describing the three aerial scenarios and the channel model. Section 3 covers the numerical results, whereas the conclusions and future work is provided in Section 4.

2. SYSTEM MODEL

In this paper, we consider three aerial vehicle communication scenarios as special instances of aerial communications over the broadband (1-1000) GHz: LAP-to-HAP scenario, HAP-to-HAP scenario, and HAP-to-SAT scenario as illustrated in Fig. 1. In the first scenario, we consider LAP-to-HAP communications, where a receiver (Rx) HAP is at a fixed altitude, $h_r = 16$ km, and a transmitter (Tx) LAP, which is initially hovering at $h_t = 400$ m, starts ascending to 4 km altitude. In the second scenario, we employ HAP-to-HAP communications, where a Tx-HAP is fixed at an altitude, $h_t = 16$ km and a Rx-HAP, which is initially at $h_r = 17$ km, starts ascending in altitude up to $h_2 = 50$ km. In the third scenario, we consider HAP-to-SAT communications, where a Rx-SAT is fixed at an altitude $h_r = 100$ km, and a Tx-HAP is initially set at $h_t = 16$ km, followed by a vertically-upward movement up to $h_t = 50$ km. Having presented the system model, in the following, we provide the channel model, which is required to analyze the total path loss and total usable bandwidth of the three considered 6G non-terrestrial communication scenarios.

2.1 Channel model

2.1.1 Total path loss

Over the considered broadband, i.e., (1-1000) GHz, the THz band is highly frequency-selective due to the molecular absorption loss contributions on top of the spreading loss. This absorption loss is caused by various gases present in the atmosphere, mainly water vapors. Absorption loss occurs when an EM wave interacts with gas molecules in the atmosphere and transfers a part of its energy to them. The absorption loss that an electromagnetic wave of frequency, f experiences at distance, d , and between Tx and Rx altitudes h_t and h_r , respectively can be expressed as:

$$A_{abs}(f, d, h_t, h_r) = e^{k(f)d}, \quad (1)$$

where $k(f)$ is the absorption coefficient, which can be obtained using various tools including HITRAN on the web [20], an atmospheric tool [21], LBLRTM [22], and ITU model [23].

In dB,

$$A_{abs}(f, d, h_t, h_r)[dB] = k(f)d10\log_{10}e. \quad (2)$$

The term ‘spreading loss’ refers to the loss in free space caused by the EM wave’s attenuation as it travels through

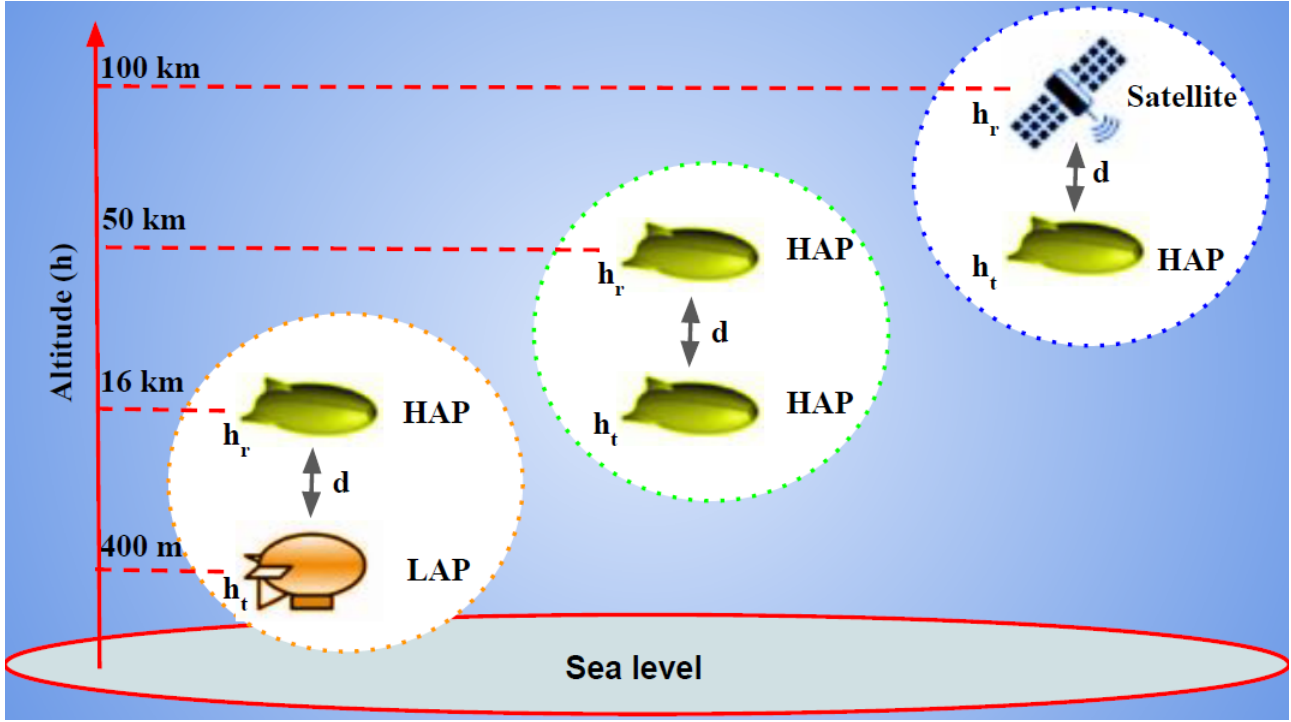


Fig. 1 – LAP-to-HAP, HAP-to-HAP and HAP-to-SAT scenarios considered in the paper.

the atmosphere via an isotropic antenna. Mathematically [7], [8]:

$$A_{spread}(f, d)[dB] = 20 \log_{10} \left(\frac{4\pi f d}{c} \right), \quad (3)$$

where c is the speed of light, which is 299,792,458 m/s.

The total path loss can be mathematically determined as the addition (in dB) of the spreading loss and absorption loss [7], [8].

$$A_{total}(f, d, h_t, h_r) = A_{spread}(f, d) + A_{abs}(f, d, h_t, h_r), \quad (4)$$

Having computed the total path loss, in the following, we present the total usable bandwidth formulations.

2.1.2 Total usable bandwidth

We compute the total usable bandwidth for each of the three scenarios i.e., LAP-to-HAP, HAP-to-HAP, and HAP-to-SAT by evaluating the vertically-up communications. Firstly, we obtain signal-to-noise ratio (γ) as:

$$\gamma(f, d, h_t, h_r) = P_t + G_t - A_{total}(f, d, h_t, h_r) - P_n, \quad (5)$$

where P_t is the total transmit power level, $G_{total} = G_t + G_r$ is the total transmit and receiver antenna gains, A_{total} is the total path loss via (4), and P_n is the power level of noise. By referring to [24, 25], we calculate P_n by considering the bandwidth, B equal to the spectral resolution of the ITU model, which is 1 GHz. Mathematically:

$$P_n = k_B T B. \quad (6)$$

Here, k_B is to the Boltzmann constant = $1.38E - 23 \text{ m}^2 \text{ kg s}^{-2} \text{ K}^{-1}$ and T is the thermal noise temperature in Kelvin. For $T = 293 \text{ K}$, (6) becomes,

$$P_n [dBm] = -174 + 10 \log_{10} B = -84 \text{ dBm}. \quad (7)$$

This assumption holds by taking the bandwidth equal to the ITU model's spectral resolution of 1 GHz. More specifically, regardless of the total available bandwidth across the entire broadband (1-1000) GHz, we analyze multiple fractional channels, each having a bandwidth of 1 GHz [24].

For reliable communications, SNR, γ should be greater than a certain threshold SNR, γ_{th} . Numerically,

$$\gamma(f, d, h_t, h_r) \geq \gamma_{th}. \quad (8)$$

Practically, various SNR thresholds are considered for a required wireless service. For instance, for UAV detection over the 2.4 GHz band (Wi-Fi here), SNR thresholds of 10 dB and 3dB are considered in [26] for indoor and outdoor services, respectively. In [27], SNR thresholds ranging from 0 dB to 20 dB are employed to analyze the coverage area over a target outage probability for providing wireless services. Consequently, the maximum tolerable total path loss, i.e., path loss threshold, A_{total}^{th} can be found as [25, 28]:

$$A_{total}^{th} [dB] = P_{total} + G_{total} - \gamma_{th} - P_n. \quad (9)$$

Here, P_t is the total transmit power level, and $G_{total} = G_t + G_r$ is the total antenna gains (Tx and Rx combined).

The path loss threshold for the HAP-to-HAP and the HAP-to-SAT scenarios are computed using (9) by considering the total transmit power, total antenna gains, and SNR threshold level(s) as listed in Table 1 and noise power level from (7).

Table 1 – Physical parameters considered in the paper for the HAP-TO-HAP AND SAT-TO-SAT communication scenarios [29].

Symbol	Parameter	Value	Unit
P_{total}	Total transmit power	30	dBm
G_t	Transmit Antenna Gain	[0,20,40]	dBi
G_r	Receiver Antenna Gain	[0,20,40]	dBi
γ_{th}	SNR Threshold	10	dB
P_n	Noise Power	-84	dBm

It can be noted here that small-scale fading is not considered in this work due to the scarcity of reflectors and scatters at the altitudes considered for LAPs, HAPs, and satellites. These reflectors and scatters, which are mainly present at ground/sea level, cause the receiver to detect multiple versions of the transmitted signal, causing distortions in phase, angle of arrival, and amplitude [30]. However, as a future extension to this work, for instance, for a LAP/HAP-ground communication scenario, small-scale fading can be incorporated as considered in [31]. Furthermore, since the THz-carrier frequencies require razor-sharp beams, hovering/cruising LAPs, HAPs, and orbiting satellites need to be precisely aligned via beam-forming [32, 33], which is also left as future work. Finally, the total usable bandwidth (B_{total}) is obtained as [25]:

$$B_{total} = \sum_j B_j, \forall j \text{ where } A_{total} < A_{total}^{th}. \quad (10)$$

Here, B_j is the usable bandwidth across j^{th} band having the total path loss, A_{total} less than the total path loss threshold, A_{total}^{th} . A visual illustration of obtaining the total usable bandwidth is provided in Fig. 2. Using Table 1 with 40 dBi total antenna gains, the path loss threshold, A_{total}^{th} corresponds to 144 dB. Therefore, the total usable bandwidth will be the sum of the bands that fall under this threshold, i.e., B_1 , B_2 , and B_3 as illustrated in Fig. 2. It is to be noted here that the metric of the total usable bandwidth defined in (10) has been employed in earlier works such as for THz communications at sea level [34], and in our earlier work for THz communications at various at-mospheric altitudes [8].

3. NUMERICAL RESULTS

In this section, we present the total path loss and total usable bandwidth results of the three aerial scenarios: (1) LAP-to-HAP communications, HAP-to-HAP communications, and HAP-to-SAT communications. We employ the International Telecommunication Union (ITU) standard atmospheric model using *ituatmos* function in MATLAB, which returns atmospheric

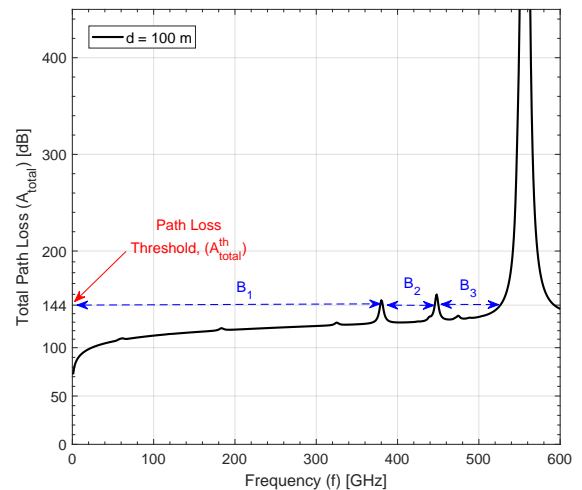


Fig. 2 – Visual illustration of total usable bandwidth over (1-600) GHz: LAP-LAP communication scenario with $h_t = 400$ m, $h_r = 500$ m, i.e., $d = 100$ m.

settings i.e., temperature, pressure, and water vapor density at a corresponding altitude [23]. Subsequently, the *gaspl* function in MATLAB is employed to compute the absorption loss for the obtained atmospheric settings [35].

3.1 LAP-to-HAP communication scenario

As our first scenario, we consider a Rx-HAP at a fixed altitude, $h_t = 16$ km, and a Tx-LAP, initially hovering at $h_r = 400$ m, starts ascending to 4 km, as shown in Fig. 1.

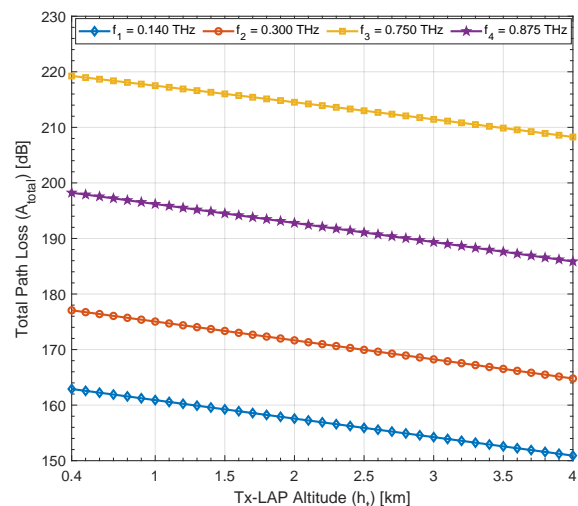


Fig. 3 – LAP-to-HAP communications: Total path loss as a function of altitude.

For the LAP-to-HAP scenario, Fig. 3 depicts the total path loss as a function of the Tx-LAP altitude (h_t here) at the four considered carrier frequencies i.e., $f_1 = 0.140$ THz (D band), $f_2 = 0.300$ THz, $f_3 = 0.750$ THz, and $f_4 = 0.875$ THz. At all four frequencies, the total path loss follows a linearly decreasing trend with respect to the Tx-LAP altitude from 400 m to 4 km, which is due to the improved atmospheric conditions at higher altitudes i.e., lower absorption loss

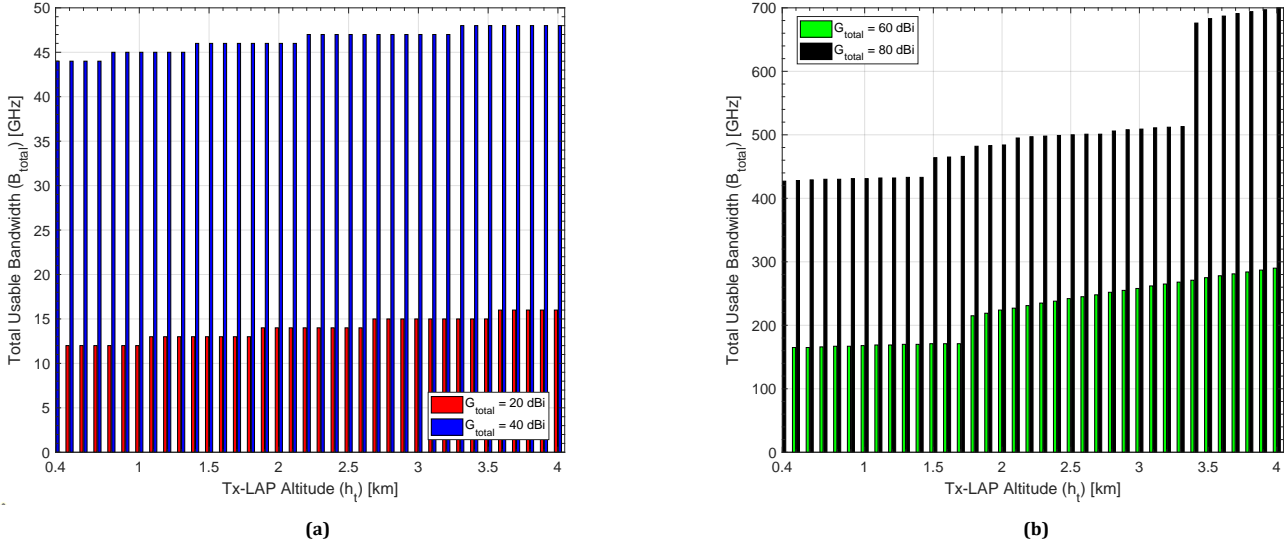


Fig. 4 – LAP-to-HAP communications: Total usable bandwidth as a function of altitude with total antenna gains: (a) 20 dBi and 40 dBi, (b) 60 dBi and 80 dBi.

(and spread loss) as compared to the lower altitudes. For instance, at $h_t = 400$ m, f_1 offers a total path loss of 162.5 dB, which decreases to 151 dB at $h_t = 4$ km altitude. Additionally, over the entire range of h_t from 400 m to 4 km, $f_3 = 0.750$ THz offers larger total path loss values as compared to a lower carrier frequency, $f_4 = 0.875$ THz. This shows the altitude and distance-based frequency-selective nature of the THz band [4]. All in all, the total path loss results in Fig. 3 showcase that the communications at practically feasible carrier frequencies over the broadband (1-1000) GHz can promise high-speed LAP-to-HAP communications as a back-haul in, e.g., Space-Air-Ground Integrated Networks (SAGINs) [36]. Fig. 4(a) shows the total usable bandwidth as a function of Tx-LAP altitude corresponding to the total antenna gains of 20 dBi and 40 dBi for the LAP-to-HAP scenario. Conversely to the trend of larger total path loss values at higher TX-LAP altitudes as in Fig. 3, here, the total usable bandwidth follows an increasing trend with altitude. For instance, with 20 dBi total antenna gains, the usable bandwidth increases from 12 GHz to 16 GHz. A similar trend can be observed for the 40 dBi gains. Fig. 4(b) depicts the total usable bandwidth vs. Tx-LAP altitude for 60 dBi and 80 dBi total antenna gains. Higher gains promise larger usable bandwidths. For instance, with 80 dBi, the total usable bandwidth varies from 420 GHz to 700 GHz as the Tx-LAP ascends from 400 m to 4 km. The results in Fig. 4 highlight the potential of employing the LAP-HAP communication over broadband (1-1000) GHz, promising LAP-HAP links in the order of 100s of Gbps.

3.2 HAP-to-HAP communication scenario

As our second scenario, we consider the Tx-HAP at a fixed altitude, $h_t = 16$ km, whereas the Rx-HAP, which is set to be at an initial altitude, $h_r = 17$ km, ascends vertically up to 50 km, as illustrated in Fig. 1.

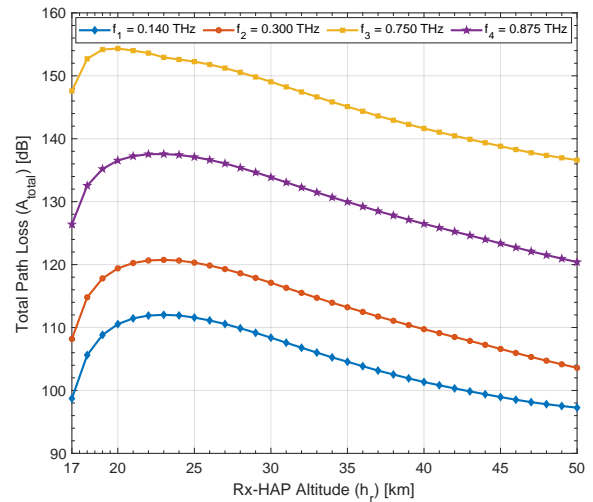


Fig. 5 – HAP-to-HAP communications: Total path loss as a function of altitude.

Fig. 5 shows the total path loss as a function of the Rx-HAP altitude (h_r , here) at the four selected frequencies i.e., $f_1 = 0.140$ THz (D band), $f_2 = 0.300$ THz, $f_3 = 0.750$ THz, and $f_4 = 0.875$ THz. At all four frequencies, the total path loss follows an increasing trend up to 22-23 km, which drops exponentially afterward up to $h_r = 50$ km altitude. This can be explained by the fact that due to reduced water vapor concentrations above 23 km altitude, the absorption loss contributions to the total path loss decline, which decreases the total path loss substantially. Interestingly, the results in Fig. 5 show that due to improved atmospheric conditions particularly above 23 km altitudes, HAP-to-HAP communications at the four considered practical carrier frequencies between 16 km to 17 km ($d = 1$ km) exhibit lower total path loss values

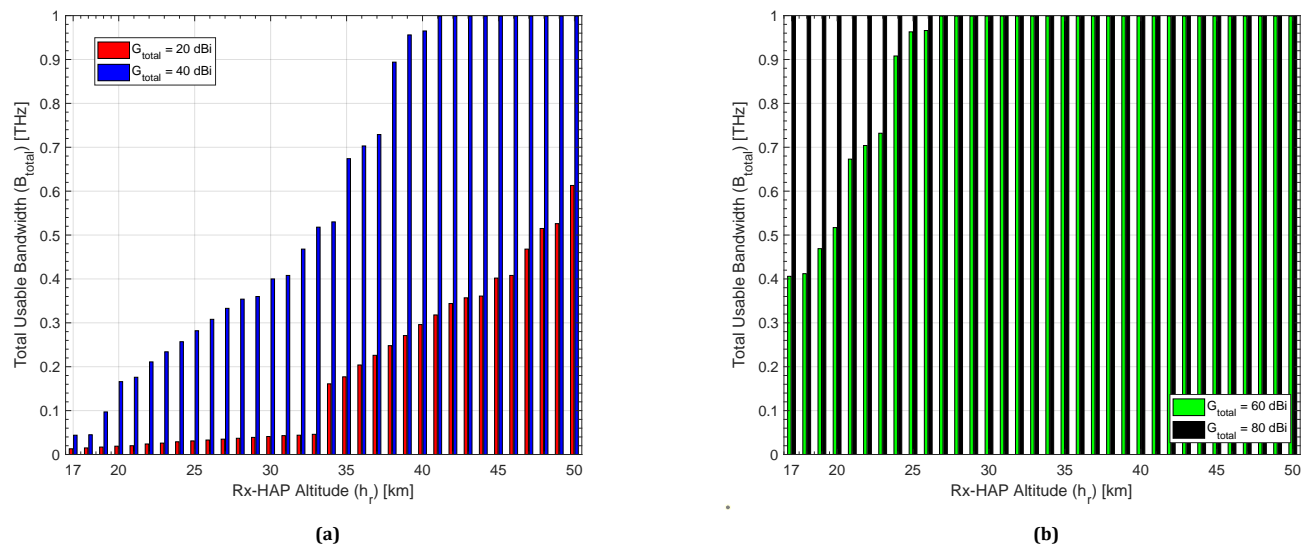


Fig. 6 – HAP-to-HAP communications: Total usable bandwidth as a function of altitude with total antenna gains: (a) 20 dBi and 40 dBi, (b) 60 dBi and 80 dBi.

as compared to the HAP-to-HAP communications between 16 km to 50 km ($d = 34$ km). More specifically, at Rx-HAP altitude of 17 km, f_1 , f_2 , f_3 , and f_4 incur the total path loss values of 98.5 dB, 108 dB, 148 dB, and 126 dB, respectively, whereas, at Rx-HAP altitude of 50 km, the respective the total path loss values are 97 dB, 104 dB, 136.5 dB, and 120 dB. Conclusively, it can be inferred that by increasing the Rx-HAP altitude i.e., increasing the altitude of the Tx-Rx-HAP communication link, a lower total path loss, up to 7.7 % is guaranteed even by increasing the Tx-Rx-HAP distance from 1 km to 34 km, promising high rate HAP-HAP communications for future 6G networks [37, 38]. Fig. 6(a) shows the total usable bandwidth over the broadband (1-1000) GHz at each Rx-HAP altitude with the total antenna gains of 20 dBi and 40 dBi. Using 40 dBi total antenna gains, the entire considered broadband (1-1000) GHz is usable at the Rx altitude of 41 km and higher. For the larger total antenna gains as shown in Fig. 6(b), the entire broadband (1-1000) GHz becomes usable starting the Rx-HAP altitudes of 27 km and 17 km with the total antenna gains of 60 dBi and 80 dBi, respectively. This showcases the true potential of employing broadband THz communications for HAP-to-HAP scenarios offering large bandwidths and Tbps links [4].

3.3 HAP-to-SAT communication scenario

As our third scenario, we consider the Rx satellite, Rx-SAT at $h_r = 100$ km, while the Tx-HAP ascends from $h_t = 16$ km up to 50 km shown in Fig. 1. Fig. 7 shows the total path loss as a function of the Tx-HAP altitude for the HAP-to-SAT scenario. Here, the total path loss decays linearly as the Tx-HAP's altitude increases. This is because, at higher atmospheric altitudes and long communication ranges i.e., at HAP altitudes from 16 km to 50 km up to the orbital satellites at 100 km

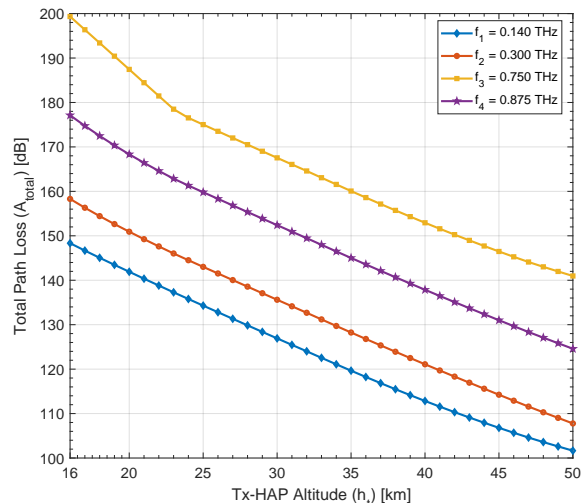


Fig. 7 – HAP-to-SAT communications: Total path loss as a function of altitude.

altitude, the water vapor concentration becomes negligible [4]. Therefore, it is mainly the spread loss affecting the EM wave propagation across the atmosphere. Fig. 7 show that all of the four considered THz carrier frequencies become feasible as the Tx-HAP's altitude increases, which can be employed for HAP-SAT links in the order of several 10s or even 100s of Tbps.

Fig. 8(a) illustrates the total usable bandwidth trend as a function of the Tx-HAP altitude for the HAP-to-SAT scenario. With both the 20 dBi and 40 dBi gains, the total usable bandwidth starts broadening exponentially with an increase in Tx-HAP altitude. For instance, on reaching 45 km altitude, even 40 dBi total antenna gains offer a total usable bandwidth of the entire considered broadband i.e., (1-1000) GHz. For the higher total antenna gains of 60 dBi and 80 dBi as considered in Fig.8(b), the entire

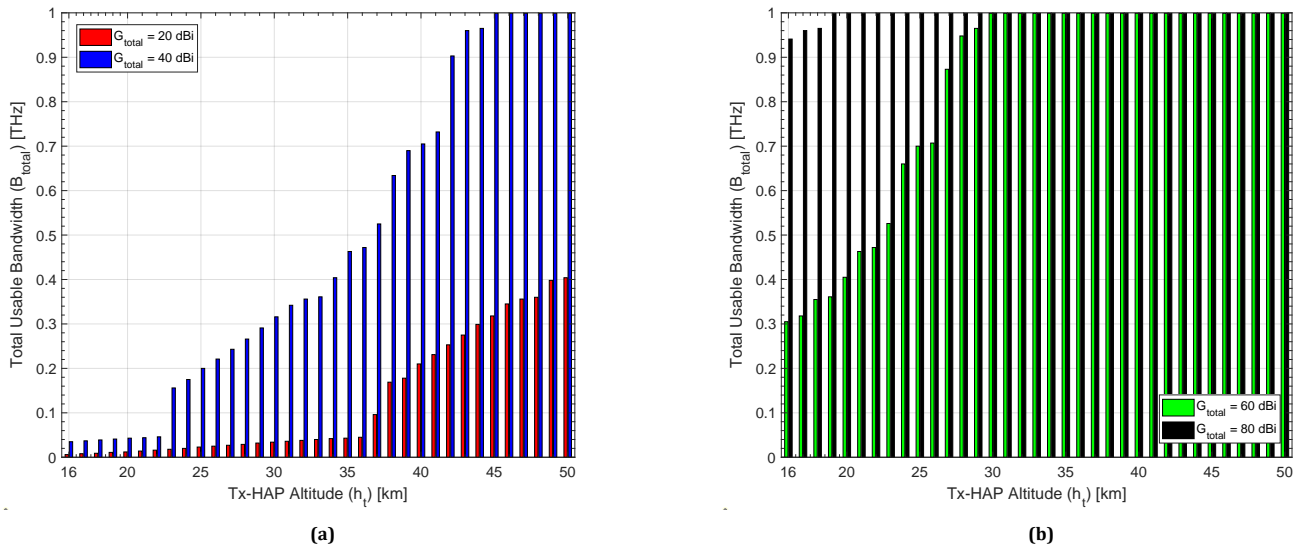


Fig. 8 – HAP-to-SAT communications: Total usable bandwidth as a function of altitude with total antenna gains: (a) 20 dBi and 40 dBi, (b) 60 dBi and 80 dBi.

broadband becomes usable even for Tx-HAP altitude = 30 km and 19 km, respectively, provisioning high rate broad-band HAP-to-SAT links in the order of 100s of Tbps [4, 39].

4. CONCLUSIONS

In this paper, we have analyzed GHz-THz broadband communications over (1-1000 GHz) in terms of total path loss and total usable bandwidth for LAP-to-HAP, HAP-to-HAP, and HAP-to-SAT scenarios. The ITU model has been employed for obtaining realistic absorption loss values at practical altitudes and ranges. The total path loss analysis exhibit that due to reduced water vapor concentrations particularly above 23 km altitudes, increasing the Rx-HAP altitude in HAP-to-HAP communications promises a lower total path loss of up to 7.7 % even at the cost of an increase in the Tx-Rx-HAP distance from 1 km to 34 km, promising Tbps rates for 6G non-terrestrial communication networks. For all three aerial communication scenarios, $f_4 = 0.875$ THz offers a lower total path loss as compared to $f_3 = 0.750$ THz due to the frequency-selective nature of the THz band. Total usable bandwidth analysis shows that with the total antenna gains of 80 dBi, bandwidth in the order of 100s of GHz is usable for the LAP-to-HAP scenario, whereas the entire considered broadband (1-1000) GHz becomes usable for the HAP-to-HAP scenario between 16 km to 50 km, and the HAP-to-SAT scenario between a HAP at 19 km and SAT at 100 km, truly showcasing the potential of employing GHz-to-THz broadband communications cognitively over (1-1000)

GHz for various practical non-terrestrial communications including LAP-to-HAP, HAP-to-HAP, and HAP-to-SAT links. Future work will include considering various other practical aerial vehicle communication scenarios under different weather profiles of the ITU model and also considering slant

directions across the atmosphere between communicating LAPs, HAPs, and satellites.

5. ACKNOWLEDGEMENT

This study is funded in part by The Scientific and Technological Research Council of Turkey within TUBITAK-BIDEB 2210-A.

REFERENCES

- [1] L. Bariah, L. Mohjazi, S. Muhaidat, P. C. Sofotasios, G. K. Kurt, H. Yanikomeroglu, and O. A. Dobre, "A Prospective Look: Key Enabling Technologies, Applications and Open Research Topics in 6G Networks," *IEEE Access*, vol. 8, pp. 174 792–174 820, 2020.
- [2] S. Kamalijam, A. Arvandi, M. Ashtarayeh, B. Safaei, and A. M. Hosseini Monazzah, "A Novel LNA Circuit in the L Band with the Purpose of Increasing Gain in GSM & GPS in Wireless Multi-Receiver Systems," in *2019 2nd International Conference on Communication Engineering and Technology (ICCET)*, 2019, pp. 112–116.
- [3] A. Saeed and O. Gurbuz, "Joint Power and Beamwidth Optimization for Full Duplex Millimeter Wave Indoor Wireless Systems," in *2019 IEEE Wireless Communications and Networking Conference (WCNC)*, 2019, pp. 1–6.
- [4] A. Saeed, O. Gurbuz, A. O. Bicen, and M. A. Akkas, "Variable-Bandwidth Model and Capacity Analysis for Aerial Communications in the Terahertz Band," *IEEE Journal on Selected Areas in Communications*, pp. 1–1, 2021.

- [5] I. F. Akyildiz, C. Han, Z. Hu, S. Nie, and J. M. Jornet, "Terahertz Band Communication: An Old Problem Revisited and Research Directions for the Next Decade," *IEEE Transactions on Communications*, vol. 70, no. 6, pp. 4250–4285, 2022.
- [6] I. F. Akyildiz, J. M. Jornet, and C. Han, "Terahertz Band: Next Frontier for Wireless Communications," *Physical Communication*, vol. 12, p. 16–32, Sep. 2014.
- [7] J. M. Jornet and I. F. Akyildiz, "Channel Modeling and Capacity Analysis for Electromagnetic Wireless Nanonetworks in the Terahertz Band," *IEEE Trans. Wireless Communications*, vol. 10, no. 10, pp. 3211–3221, 2011. [Online]. Available: <https://doi.org/10.1109/TWC.2011.081011.100545>
- [8] A. Saeed, O. Gurbuz, and M. A. Akkas, "Terahertz Communications at Various Atmospheric Altitudes," *Physical Communication*, vol. 41, p. 101113, 2020.
- [9] M. Civas, T. Yilmaz, and O. Akan, "Terahertz Band Intersatellite Communication Links," *In Next Generation Wireless Terahertz Communication Networks*, pp. 337–354, 06 2021.
- [10] K. Tekbiyik, A. R. Ekti, G. Karabulut-Kurt, A. Görçin, and H. Yanikomeroglu, "A Holistic Investigation on Terahertz Propagation and Channel Modeling Toward Vertical Heterogeneous Networks," *ArXiv*, vol. abs/2005.00509, 2020.
- [11] J. Kokkonen, J. M. Jornet, V. Petrov, Y. Koucheryavy, and M. Juntti, "Channel Modeling and Performance Analysis of Airplane-Satellite Terahertz Band Communications," *IEEE Transactions on Vehicular Technology*, vol. 70, no. 3, pp. 2047–2061, 2021.
- [12] M. Civas and O. B. Akan, "Terahertz Wireless Communications In Space," *ITU Journal on Future and Evolving Technologies*, vol. 2, no. 7, pp. 31–38, 2021.
- [13] A. Saeed, O. Gurbuz, and Akkas, "Terahertz Band Communications As A New Frontier For Drone Networks," *ITU Journal on Future and Evolving Technologies, Terahertz communications*, vol. 2, no. 7, pp. 1–19, 2021.
- [14] C. Han and I. F. Akyildiz, "Distance-Aware Bandwidth-Adaptive Resource Allocation for Wireless Systems in the Terahertz Band," *IEEE Transactions on Terahertz Science and Technology*, vol. 6, no. 4, pp. 541–553, 2016.
- [15] M. Yu, A. Tang, X. Wang, and C. Han, "Joint Scheduling and Power Allocation for 6G Terahertz Mesh Networks," in *2020 International Conference on Computing, Networking and Communications (ICNC)*, 2020, pp. 631–635.
- [16] B. E. Y. Belmekki and M.-S. Alouini, "Unleashing the Potential of Networked Tethered Flying Platforms: Prospects, Challenges, and Applications," *IEEE Open Journal of Vehicular Technology*, vol. 3, pp. 278–320, 2022.
- [17] J. Kokkonen, J. Lehtomäki, and M. Juntti, "A Line-of-Sight Channel Model for the 100–450 Gigahertz Frequency Band," *EURASIP Journal on Wireless Communications and Networking*, vol. 2021, no. 1, pp. 1–15, 2021.
- [18] M. Erdem, A. Saleem, O. Gurbuz, C. Ecemis, and A. Saeed, "A Simple Analytical Model for Thz Band Path Loss," *IEEE Communications Letters*, pp. 1–1, 2023.
- [19] A. Saeed, A. Saleem, O. Gurbuz, and M. A. Akkas, "Characterization of Terahertz Band Transmittance from Sea-level to Drone Altitudes," in *2021 International Balkan Conference on Communications and Networking (BalkanCom)*, 2021, pp. 152–156.
- [20] "Hitran on the Web." [Online]. Available: <http://hitran.iao.ru/>
- [21] S. Paine, "The am Atmospheric Model," Sep. 2019. [Online]. Available: <https://www.cfa.harvard.edu/~spaine/am/>
- [22] S.A. Clough , M.W. Shephard , E.J. Mlawer , J.S. Delamere , M.J. Iacono , K. Cady-Pereira , S. Boukabara and P.D. Brown, "Atmospheric Radiative Transfer Modeling: a Summary of the AER Codes," *Journal of Quantitative Spectroscopy and Radiative Transfer*, vol. 91, no. 2, pp. 233 – 244, 2005. [Online]. Available: <http://www.sciencedirect.com/science/article/pii/S0022407304002158>
- [23] ITU, "Reference Standard Atmospheres," *Recommendation ITU-R P.835-6, P Series, Radiowave Propagation*, no. P.835-6, December 2017.
- [24] T. Schneider, A. Wiatrek, S. Preussler, M. Grigat, and R. Braun, "Link Budget Analysis for Terahertz Fixed Wireless Links," *IEEE Transactions on Terahertz Science and Technology*, vol. 2, no. 2, pp. 250–256, March 2012.
- [25] C. Han, A. O. Bicen, and I. F. Akyildiz, "Multi-Wideband Waveform Design for Distance-Adaptive Wireless Communications in the Terahertz Band," *IEEE Transactions on Signal Processing*, vol. 64, no. 4, pp. 910–922, Feb 2016.
- [26] W. Nie, Z.-C. Han, M. Zhou, L.-B. Xie, and Q. Jiang, "Uav detection and identification based on wifi signal and rf fingerprint," *IEEE Sensors Journal*, vol. 21, no. 12, pp. 13 540–13 550, 2021.

- [27] M. M. Azari, F. Rosas, K.-C. Chen, and S. Pollin, "Optimal uav positioning for terrestrial-aerial communication in presence of fading," in *2016 IEEE Global Communications Conference (GLOBECOM)*, 2016, pp. 1–7.
- [28] M. Alzenad, A. El-Keyi, and H. Yanikomeroglu, "3-d placement of an unmanned aerial vehicle base station for maximum coverage of users with different qos requirements," *IEEE Wireless Communications Letters*, vol. 7, no. 1, pp. 38–41, 2018.
- [29] J. L. Zhendong Yin, Zhenguo Shi and Z. Wu, "Design of Unmanned Aerial Vehicle Space Communication Links Based on DS-UWB," *Information Technology Journal*, vol. 9, no. 9, pp. 1713–1718, 2010.
- [30] A. Goldsmith, *Wireless Communications*. New York, NY, USA: Cambridge University Press, 2005.
- [31] F. Dovis, R. Fantini, M. Mondin, and P. Savi, "Small-Scale Fading for High-Altitude Platform (HAP) Propagation Channels," *IEEE Journal on Selected Areas in Communications*, vol. 20, no. 3, pp. 641–647, 2002.
- [32] S. Krishna Moorthy and Z. Guan, "Beam Learning in Mmwave/THz-band Drone Networks Under In-Flight Mobility Uncertainties," *IEEE Transactions on Mobile Computing*, pp. 1–1, 2020.
- [33] Z. Guan and T. Kulkarni, "On the Effects of Mobility Uncertainties on Wireless Communications between Flying Drones in the mmWave/THz Bands," in *IEEE INFOCOM 2019 - IEEE Conference on Computer Communications Workshops (INFOCOM WKSHPS)*, 2019, pp. 768–773.
- [34] C. Han, A. O. Bicen, and I. F. Akyildiz, "Multi-Wideband Waveform Design for Distance-Adaptive Wireless Communications in the Terahertz Band," *IEEE Transactions on Signal Processing*, vol. 64, no. 4, pp. 910–922, Feb 2016.
- [35] ITU, "Attenuation by Atmospheric Gases 2013," *Radiocommunication Sector of International Telecommunication Union. Recommendation ITU-R P.676-10*, no. P.676-10, 2013.
- [36] A. Liao, Z. Gao, D. Wang, H. Wang, H. Yin, D. W. K. Ng, and M.-S. Alouini, "Terahertz Ultra-Massive MIMO-Based Aeronautical Communications in Space-Air-Ground Integrated networks," *IEEE Journal on Selected Areas in Communications*, vol. 39, no. 6, pp. 1741–1767, 2021.
- [37] N. Saeed, H. Almorad, H. Dahrouj, T. Y. Al-Naffouri, J. S. Shamma, and M.-S. Alouini, "Point-to-Point Communication in Integrated Satellite-Aerial 6G Networks: State-of-the-Art and Future Challenges," *IEEE Open Journal of the Communications Society*, 2021.
- [38] Z. Jia, M. Sheng, J. Li, and Z. Han, "Towards Data Collection and Transmission in 6G Space-Air-Ground Integrated Networks: Cooperative HAP and LEO Satellite Schemes," *IEEE Internet of Things Journal*, 2021.
- [39] J. Y. Suen, M. T. Fang, S. P. Denny, and P. M. Lubin, "Modeling of Terabit Geostationary Terahertz Satellite Links from Globally Dry Locations," *IEEE Transactions on Terahertz Science and Technology*, vol. 5, no. 2, pp. 299–313, March 2015.

AUTHORS



Akhtar Saeed received his B.E. degree in telecommunications engineering from U.I.T Hamdard University in 2010 and his M.E. degree in telecommunications engineering from NED University of Engineering and Technology in 2014. He received his Ph.D. degree in electronics engineering from Sabanci University in 2021 under the supervision of

Dr Ozgur Gurbuz and the co-supervision of Dr Mustafa Alper Akkaş. He is currently associated as an Assistant Professor at the Department of Electrical Engineering, DHA Suffa University, Karachi, Pakistan. His research interests include body area networks, molecular communications, the internet of things, terahertz communications at various atmospheric altitudes, millimeter wave communications, wireless sensor networks, and full duplex communications.



Hilal Esra Yıldız is a graduate student at Boğaziçi University, Electrical and Electronics Engineering. She also works at Hava Elektronik Sanayi A.Ş. (HAVELSAN) as a software engineer. She received her undergraduate degree from Yıldız Technical University, Electronic and Communication Engineering. Her research focuses on

UWB indoor positioning and Terahertz Band communications.



Fatih Alagoz is a professor in the Department of Computer Engineering, Bogazici University. He received a B.Sc. degree in Electrical Engineering from the Middle East Technical University, Turkiye, in 1992, and M.Sc. and D.Sc. degrees in Electrical Engineering from The

George Washington University, USA, in 1995 and 2000, respectively. His current research areas include wireless/mobile/satellite networks, network security, and communications. He has contributed to many research projects for the US Army of Intelligence Center, Naval Research Laboratory, UAE Research Fund, Turkish Scientific Research Council, State Planning Organization of Turkey, BAP, etc. He has published scores of scholarly papers in selected journals and conferences.